

# Parsimonious modeling for estimating hospital cooling demand to improve energy efficiency

Eduardo Dulce-Chamorro<sup>a</sup>, Francisco Javier Martinez-de-Pison<sup>a,\*</sup>

<sup>a</sup> *EDMANS Group, Department of Mechanical Engineering, University of La Rioja, Logroño, Spain.*

---

## Abstract

Of all the different types of public buildings, hospitals are the biggest energy consumers. Cooling systems for air conditioning and healthcare uses are particularly energy-intensive. Forecasting hospital thermal-cooling demand is a remarkable and innovative method capable of improving the overall energy efficiency of an entire cooling system. Predictive models allow users to forecast the activity of water-cooled generators and adapt power generation to the real demand expected for the day ahead, while avoiding inefficient subcooling. In addition, the maintenance costs related to unnecessary starts and stops and power-generator breakdowns occurring over the long-term can be reduced.

This study is based on the operations of a real hospital facility and details the steps taken to develop an optimal and efficient model based on a genetic methodology that searches for low-complexity models through feature selection, parameter tuning and parsimonious model selection. The methodology, called *GAparsimony*, has been tested with neural networks, support vector machines and gradient boosting techniques. Finally, a weighted combination of the three best models was created.

The new operational method employed herein can be replicated in similar buildings with similar water-cooled generators.

*Keywords:* *GAparsimony*, parsimonious modeling, hybrid forecasting, thermal demand forecasting, cooling demand forecasting, Building Management System, Air Conditioning.

---

## 1. Introduction

Hospitals require vast amounts of energy. In particular hospital cooling systems that use chilled water for air conditioning (AC) or in other essential healthcare services and activities are what make hospitals some of the most energy-intensive consumers.

A common pitfall in many facilities is that after equipment is installed, it is not set up according to the expected level of energy efficiency. Using Building Management Systems (BMS) can improve energy efficiency and generate economic savings [1, 2]. Hospitals can decrease their energy use by 20% to 30% by implementing a BMS, adequately zoning for AC, using temperature measurement and control systems in different areas and planning proper-use schedules, and regulating the speeds of fans and water pumps [3].

---

\*Corresponding author

Email address: [fjmartin@unirioja.es](mailto:fjmartin@unirioja.es) (Francisco Javier Martinez-de-Pison)

11 The BMS used herein this study was implemented during the construction of the hospi-  
12 tal under study in January 2008. The existing BMS, like most systems installed in buildings,  
13 is based on real-time control that utilizes information captured by sensors. Nevertheless,  
14 the control system generated more starts and stops than necessary in the liquid-cooled gen-  
15 erators. This led to premature ageing in the generators, higher cooling demand than neces-  
16 sary, frequent breakdowns, and unnecessary thermal variations that did not correspond to  
17 the actual demand.

18 This study addresses these problems and improves the building’s overall efficiency by  
19 creating a predictive model of the thermal cooling demand to help forecast the activity of  
20 the hospital’s water-cooled generators (controlled by the BMS).

### 21 1.1. *The Search for Parsimonious Models*

22 Several prior studies have already conducted related research into energy efficiency:  
23 Analysis of building energy consumption in a hospital [4], forecasting cooling demand  
24 [5, 6] and short-term electrical load [7, 8]. These studies often utilize Gaussian processes  
25 [9], support vector machines(SVM) [10, 11], artificial neural networks (ANN) [12, 13], ANN  
26 applied to electrical consumption forecasting in a hospital facility [14], ANN comparison  
27 with random forest (RF) [15], and hybrid methods [16].

28 Forecasting applications are often based on regression models that are constructed with  
29 small databases gathered over a short period of time. In this case, however, the information  
30 was collected over more than three years, and during this period substantial improvements  
31 were achieved in the control of the cooling system. Therefore, the training database could  
32 be reduced to include just the final 21 months. In addition, the pre-processing strategy  
33 adopted measurements averaged by the hour, thereby considerably reducing the size of  
34 the training dataset and translating energy data to a common and understandable unit (in  
35 kWh).

36 In this kind of situation, seeking out low-complexity models (that is, more parsimonious  
37 models), among various accurate solutions, is usually a reliable strategy for finding models  
38 that are robust against perturbations or noise. Parsimonious models aim to have a lower  
39 number of features, making them easier to maintain and understand [17, 18].

40 In recent years, there is an increasing need to create methods to automate and facilitate  
41 modeling processes with hyperparameter optimization (HO), and feature selection (FS),  
42 in order to reduce the human effort involved in these time-consuming tasks [19, 20] and  
43 therefore allow researchers to focus on other important processes like feature engineering  
44 or data mugging. Among the currently available methods, GAparsimony [21] is a genetic  
45 algorithm (GA) methodology that searches for parsimonious models and is specifically de-  
46 signed to work with smaller datasets. GAparsimony optimizes HO and FS by executing a  
47 parsimonious model selection (PMS), which is based on criteria that considers complex-  
48 ity and accuracy separately. Although GAparsimony performs quite well with HO, model  
49 selection with a complexity measurement based on the number of selected features has  
50 proven to be useful for obtaining more parsimonious solutions as compared to previous  
51 experiments [22].

52 GAparsimony has been extremely useful with classical machine learning methods, such  
53 as extreme gradient boosting machines (XGBoost), support vector regression (SVR), ran-  
54 dom forest (RF) or artificial neural networks (ANNs) [23], and has also been successfully  
55 applied in a range of contexts such as steel industrial processes [24], hotel room booking  
56 forecasting [25], mechanical [26] design and solar radiation forecasting [27]. The GAparsimony  
57 package for R has been available since July 2017 [28].

58 The present study presents a real application of GAparsimony that was utilized to create  
59 a parsimonious predictive model of a hospital's cooling demand. With the model created  
60 in this research, the amount of cooling water generated can be adapted to meet the actual  
61 demand expected for the day ahead, meanwhile maintenance costs related to power gen-  
62 erator breakdowns or ineffective starts and stops can also be reduced. Thus, the model can  
63 be useful for improving overall energy efficiency, decreasing the electrical consumption of  
64 cooling systems and CO<sub>2</sub> emissions, and minimizing maintenance costs.

## 65 2. Case study description

66 The San Pedro Hospital is located in the city of Logroño (Spain), It is the top hospi-  
67 tal in the autonomous community of La Rioja, and is part of the Spanish national public  
68 healthcare system.

69 The building covers an area of about 125,000 m<sup>2</sup>. Most of the thermal generation, gas  
70 and high voltage installations are located in a separate building. Let us make note of the  
71 most energy-intensive medical services offered by this hospital: 600+ beds for hospital-  
72 ization, a diagnostic imaging area, 23 operating rooms, emergency and consultation area  
73 with 21 boxes, hemodialysis, an intensive care unit, endoscopy, rehabilitation, laboratories,  
74 pharmacy, sterilization, and other general services.

### 75 2.1. Description of the installations

76 The San Pedro hospital has a centralized cold-water production system for the high  
77 cooling demand of many healthcare services and for air conditioning the building. The  
78 system consists of 4 chillers EF1, EF2, EF3 and EF4: 3 centrifugal units of 3.51 MW (*Trane*  
79 *CVFG* equipment), and 1 screw machine with 1 MW (*Trane RTHD* equipment) of cooling  
80 capacity. The system's electrical consumption data is described in Table 1.

81 The hospital's BMS is comprised primarily by controllers belonging to the Sauter Sauter  
82 *EY3600* family, which communicate with each other through the *novaNet* bus. The Building  
83 Management System is a SCADA application with a *novaPro Open 4.1*. environment. The  
84 server is located in the hospital data center.

85 Chilled water in a hospital has essential applications not only for human welfare, but  
86 also for industrial and healthcare needs: air conditioning operating rooms, out-patient  
87 surgery, intensive care, delivery rooms, and emergency rooms, for example. It is also uti-  
88 lized in radiology and diagnostic imaging equipment, scanners, mammography, etc.; and  
89 for refrigeration storage such as in a blood bank, kitchen, or pharmacy; for Kardex, patho-  
90 logical anatomy, and in the morgue, laboratories, and data center racks, etc.

91 This article focuses on the study of a prediction model for a chilled-water system, given  
92 its significance for hospital services and its significant electrical consumption. Specific stud-  
93 ies of hospitals have shown that the energy they use to generate chilled water exceeds 45%  
94 of the total energy necessary for building operations [3].

### 95 2.2. Optimization process for the cooling system

96 The existing problems detected in the cooling water system were:

- 97 - Uncontrolled starts and stops of the cooling generators, which negatively impact en-  
98 ergy efficiency and can lead to significant breakdowns.

Table 1: Chilled Water production data.

	<b>Electric Power</b>	<b>Flow</b>
<b>Cooling unit with 3.5 MW of cooling power (per unit)</b>	<b>754.60 kW</b>	<b>-</b>
Centrifugal Chiller (EF1, EF2, EF3)	574.60 kW	
Group of evaporation pumps	45.00 kW	<b>615.60 m3/h</b>
Group of condensation pumps	90.00 kW	770.40 m3/h
Fans (3 units)	45.00 kW	
<b>Cooling unit with 1 MW of cooling power (total)</b>	<b>317.50 kW</b>	<b>-</b>
Screw Chiller (EF4)	280.00 kW	
Group of evaporation pumps	7.50 kW	<b>205.00 m3/h</b>
Group of condensation pumps	15.00 kW	253.00 m3/h
Fan	15.00 kW	
<b>Chilled Water circuit</b>	<b>37.00 kW</b>	<b>2019.60 m3/h</b>
Group of drive pumps (4 pumps)	9.25 kW	673.20 m3/h

99 - Subcooling water-ring temperature below established set points, is detrimental to en-  
 100 ergy efficiency.

101 - Overheating water-ring temperature above established set points, can adversely af-  
 102 fect health care processes.

103 Therefore, as a result of re-engineering and optimization using Exploratory Data Anal-  
 104 ysis (EDA) techniques and a full review of the installations, several actions were imple-  
 105 mented following an established timeline, as can be seen in Figure 1, in order to improve  
 106 the energy efficiency of the cooling system:

- 107 1. The first optimization of the system improved how the BMS calculated the temper-  
 108 ature set point of the cold-water ring to cut down on the number of starts and stops  
 109 in the chillers. This modification implemented a variable and graduated set point  
 110 depending on the outside temperature.
- 111 2. The second optimization established a minimum work-time for every generator of at  
 112 least one hour, and set up a cyclic order of use.
- 113 3. The third optimization implemented a variable setpoint for the ring temperature to  
 114 be regulated according to the outside temperature as a ramp variable instead of as a  
 115 stepped variable .
- 116 4. The fourth optimization consisted of installing frequency inverter systems in the EF4  
 117 generator. The frequency inverter (AFD) can regulate the speed of the compressor  
 118 motor with a partial load. In the EF1, EF2, EF3, which are centrifugal chillers, AFDs  
 119 could not be installed, since they still have a modulation with the refrigerant charge.  
 120 Communication hardware cards were installed in every generator to improve com-  
 121 munication with the BMS.

122 The first energy demand models were calculated in March 2019 but inefficient behav-  
 123 ior was observed following the improvements implemented in April 2018 (see Figure 3).

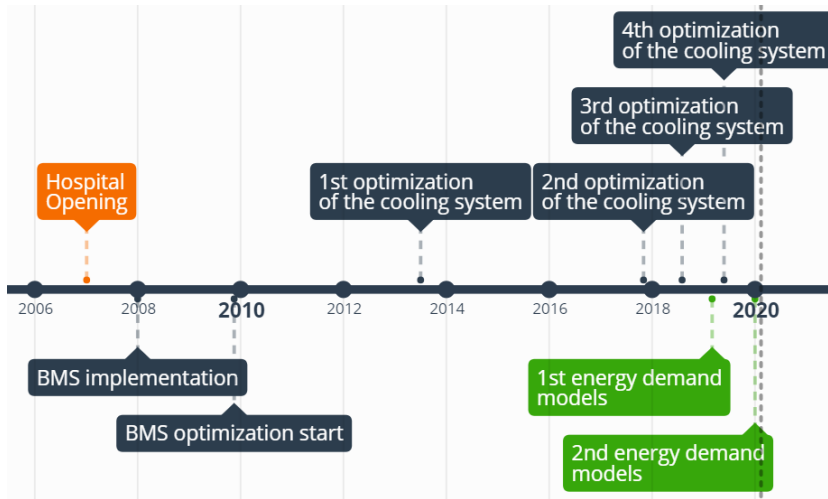


Figure 1: Case study timeline indicating remarkable improvements and model generations.

124 Therefore, the preprocessed data and the model itself needed to be updated to improve the  
 125 model's accuracy. The second set of energy demand models were calculated in January  
 126 2020 after notable improvements were applied to the real system.

### 127 3. Dataset

#### 128 3.1. Data extraction

129 The BMS installed in San Pedro Hospital recorded data through a measurement logger  
 130 in the generation system (the BMS Sauter novaPro Open). Cooling energy was not mea-  
 131 sured by the system, thus it had to be calculated and the data preprocessed. The variables  
 132 extracted from the BMS generation system are listed in Table 2.

Table 2: Control system variables

Short name	Description
EF1	EF1 - Status
EF2	EF2 - Status
EF3	EF3 - Status
EF4	EF4 - Status
TIMP	Cold Ring Drive Temperature [°C]
TEXT	Exterior Temperature of Facilities Building [°C]
TCONSIG	Calculated Setpoint of the regulation for Cold Production Drive [°C]
TENEF1 to 4	Water temperature at the inlet of the EF1 to EF4 [°C]
TSALEF1 to 4	Water temperature at the outlet of the EF1 to EF4 [°C]

133 3.2. Data preprocessing

134 Data preprocessing involved the following actions:

- 135 1. Averaging measurements by the hour. The system recorded data whenever a vari-  
136 able altered its state or changed its measurement. The time difference between mea-  
137 surements could range from seconds to hours. Therefore, the data was divided into  
138 groups and presented by the hour .
- 139 2. Filling in missing values. Imputation of missing values was done by using the mean  
140 of the previous and next values.
- 141 3. Creating *Generated Thermal Power* and ENERGYKWHPOST features.
- 142 4. Filtering the target (ENERGYKWHPOST) to create a more stable variable.

143 The BMS lacked a thermal energy meter to save and measure the data. Nevertheless,  
144 both the instantaneous thermal power and the generated thermal energy could be obtained.  
145 Thanks to the other available variables in the measurement system and the fact that the  
146 pump flow in this system has a set value, thermal power could be calculated by the follow-  
147 ing formula:

$$Thermal\ Power = Flow * Thermal\ jump * Ce \quad (1)$$

148 Where the thermal power is expressed in watts [W], the flow rate in l/h, and the ther-  
149 mal jump in the chiller in degrees Celsius [°C]. The specific heat of water is equal to 1.16  
150 Wh/kg°C and its specific weight is 1kg/l.

151 The time differences between thermal power measurements is a known value, so ther-  
152 mal energy could be calculated. Considering that the minimum work-time of generators  
153 is one hour, the chosen prediction variable was energy, ENERGYKWHPOST [kWh], rather  
154 than instantaneous power [kW].

155 Due to the previous adjustments made to remedy incorrect starts/stops and setpoints in  
156 the generators, the calculated variable of Thermal Energy (ENERGYKWHPOST) exhibited  
157 a sawtooth graph, as can be seen in Figure 3. Such results could later lead to an inade-  
158 quate learning process; and thus the thermal energy was filtered in order to smooth out  
159 ENERGYKWHPOST, as can be observed in Figure 2.

Table 3: Data filtering of prediction variable, year 2018

Filter:	ENERGY [kWh]	RMS	MAE
ENERGYKWHPOST	<b>10.266.880,7</b>	0	0
ENE_GAUSSFILT3	10.266.843,3	<b>166,4</b>	37,4
ENE_GAUSSFILT5	<b>10.266.883,6</b>	278,3	<b>2,9</b>
ENE_GAUSSFILT9	10.266.911,1	328,2	30,4
ENE_GAUSSFILT11	10.266.889,9	338,5	9,2

160 Different filters were tested, but the Gaussian function was the method selected to fil-  
161 ter and smooth thermal energy. This method was chosen for it slow error rate, as shown  
162 in Table 3, and because the accumulated energy in the tested year was similar to the real  
163 amount of accumulated energy. ENERGYKWHPOST was compared with different filters  
164 (see Figure 2). A Gaussian filter with a window size of 11 (ENE\_GAUSSFILT11), repre-  
165 sented by a dashed line, displayed a smoother curve without distortion as compared to the

166 dotted line of a Gaussian filter with a window size of 3 (ENE\_GAUSSFILT3). Therefore,  
 167 ENE\_GAUSSFILT11, was eventually selected as the target. This feature was considered  
 168 close to the hospital’s energy demand, which primarily depends upon weather conditions  
 169 and the use of the facilities.

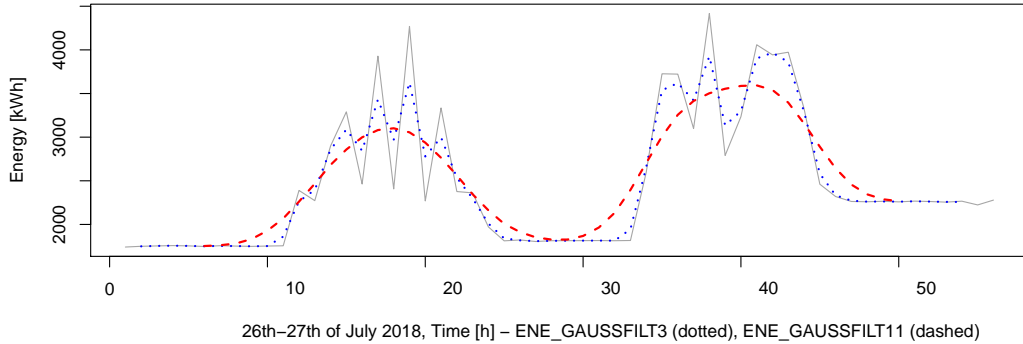


Figure 2: Filtering ENERGYKWHPOST with different Gaussian steps.

### 170 3.3. Final dataset

171 The attributes selected were the following:

Table 4: Attributes selected for the forecast model.

Variable	Description
ENE_GAUSSFILT11	Target.
month	Month of measurement.
day_of_week	Day of the week.
Is_holiday	Boolean variable for holiday.
TIMP	Instant impulsion temperature.
TEXT	Instant exterior temperature.
TMEAN	Average daily temperature.
TMAX	Maximum daily temperature.
TMIN	Minimum daily temperature.

## 172 4. Parsimonious Modeling

173 The search for parsimonious models was performed with the *GAparsimony* method-  
 174 ology. For this purpose, three popular algorithms were used: support vector machines  
 175 (SVR) with RBF kernel, artificial neural networks (ANN), and extreme gradient boosting  
 176 machines (XGB). All the experiments were implemented with the *GAparsimony* [29] pack-  
 177 age in R programming language.

### 178 4.1. *GAparsimony* settings

179 *GAparsimony* optimization extracts the algorithm’s parameters and the selected input  
 180 features from the  $\lambda_g^i$  chromosome for each individual  $i$  of the generation  $g$ .

181 Chromosome  $\lambda_g^i$  was defined for each method as:

$$\begin{aligned} SVR(\lambda_g^i) &= [cost, gamma, epsilon, Q] \\ ANN(\lambda_g^i) &= [size, decay, num\_epochs, Q] \\ XGB(\lambda_g^i) &= [subsample, colsample\_bytree, \\ &max\_depth, alpha, lambda, Q] \end{aligned} \quad (2)$$

182

183 Where the values correspond to the algorithm's parameters except the last one,  $Q$ , which is  
184 a vector of probabilities for selecting each input feature  $j$  when  $Q_j \geq 0.5$ .

185 GAparsimony uses Root Mean Squared Error (RMSE) for evaluating individuals within  
186 the optimizing process,  $RMSE_{val}$ . RMSE measured with the test database,  $RMSE_{test}$ , is used  
187 to check the model's generalization capability. Finally, model complexity reflects to the  
188 number of selected features  $N_{FS}$ . This complexity performed well in previous experiments  
189 with GAparsimony.

190 The genetic optimization process in GAparsimony is defined with a population of 40  
191 individuals evaluated in 100 generations but with an early stopping criteria if  $RMSE_{val}$   
192 does not improve in 20 iterations. The selection process uses 20% of the best solutions and  
193 is based on a two-step process: first, models are ordered by  $RMSE_{val}$ , next, individuals  
194 with similar  $RMSE_{val}$  are reordered according to complexity. The objective is to promote  
195 parsimonious solutions (with lower complexity) to top positions. In this case, two  $RMSE_{val}$   
196 are considered to be similar if their  $RMSE_{val}$  absolute difference is lower than a ReRank  
197 parameter which is defined by the user. In this study, after several experiments,  $ReRank =$   
198 0.1 achieved a satisfactory trade-off between complexity and  $RMSE_{val}$ .

199 In order to start the GA process with a high percentage of input, 90% of the features  
200 were selected from the first population. Finally, mutation was defined by the number of  
201 most elite individuals that were not mutated (2), the probability of mutation in the model's  
202 parameter in the chromosome (10%), and the probability of a feature having the value of 1  
203 if the feature is selected to be mutated (10%). This parameter was set to a low value of 10%  
204 to facilitate the reduction of input features in the following generations.

## 205 5. Results and Discussion

### 206 5.1. Initial energy-demand models

207 The first energy-demand models were trained with the dataset from the period between  
208 January 2017 and February 2018. The validation database corresponds to the even weeks  
209 between March 2018 and February 2019, and the testing database with the odd weeks of  
210 that same time period.

211 Surprisingly, GAparsimony with SVR was capable of obtaining a parsimonious model  
212 with only 3 attributes and acceptable validation and testing errors. To some degree, an  
213 explanation for this can be found in the improvements (applied) in the control process after  
214 the first acquisition period that averaged out 'the noise' thereby reducing the differences  
215 between the training database and the validation/testing data.

216 The SVR algorithm obtained the best validation and testing error with only 3 attributes:  
217 month (month), and the external (TEXT) and minimum temperatures (TMIN). ANN came  
218 in second place with 7 features and, finally, XGB which selected only 4.



219 Table 5 shows the validation and testing errors, and the final selected features for the  
 220 best model from the last generation with SVR, ANN, and XGB, respectively.

Table 5: Best individual for each algorithm obtained with `GAparsimony`.

	SVR	ANN	XGB
$RMSE_{val}$	<b>294.9</b>	327.4	347.8
$RMSE_{tst}$	<b>342.4</b>	363.3	371.1
<b>VARs:</b>			
month	1	1	1
day_of_week	0	1	1
Is_holiday	0	1	0
TIMP	0	1	1
TEXT	1	1	1
TMEAN	0	0	0
TMAX	0	1	0
TMIN	1	1	0
Complexity	<b>3</b>	7	4

## 221 5.2. Second energy-demand models

222 In order to create the second set of energy-demand models, the data recorded between  
 223 2017 to March 2018 was removed due to the significant optimizations implemented in the  
 224 cooling system during this period. Figure 3 shows the high level of noise produced by inef-  
 225 ficient starts and stops prior to April 2018. Thus, the second model was trained and tested  
 226 with the information collected from April 2018 to December 2019. The training dataset cor-  
 227 responds to the period between January 2018 and February 2019. The validation data base  
 228 corresponds to the even weeks between March 2019 and December 2019; and the testing  
 229 database to the odd weeks of the same time period.

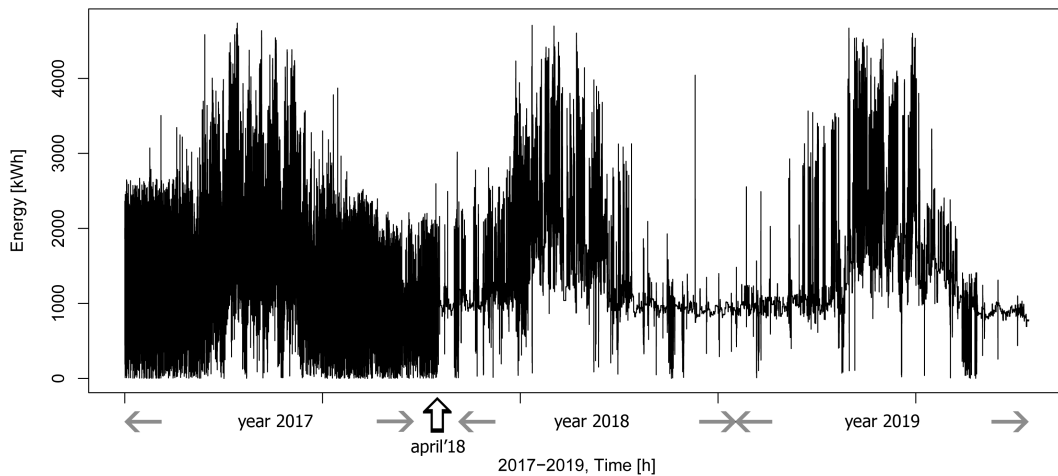


Figure 3: Evolution of ENERGYKWHPOST within the acquisition.

230 GAparsimony was used again to choose the best models among the different algorithms,  
 231 to adjust the internal parameters, and develop the feature selection as well. Errors, param-  
 232 eters, and selected features are shown in Table 6. In the table below, it can be observed that  
 233 the error values are better than those obtained with the initial energy-demand model.

Table 6: Best models with results, complexity, generation and parameters.

	SVR	ANN	XGB		
$RMSE_{val}$	<b>231.9</b>	233.2	239.8		
$RMSE_{tst}$	<b>260.9</b>	268.2	267.7		
month	1	1	1		
day_of_week	0	0	1		
Is_holiday	0	1	0		
TIMP	0	1	0		
TEXT	1	1	1		
TMED	1	1	1		
TMAX	1	0	0		
TMIN	0	0	0		
Complexity	<b>4</b>	5	<b>4</b>		
Generation	V7	V4	V4		
Parameters:					
$expcost$	0.42	$size$	21	$subsample$	0.70
$gamma$	0.20	$decay$	45.0	$colsample_bytree$	0.91
$epsilon$	0.09	$maxit$	637.8	$max\_depth$	2
				$alpha$	0.03
				$lambda$	0.31

234 **SVR Model:** The best SVR model was obtained with 4 features: month (*month*), and the  
 235 external (*TEXT*), averaged (*TMED*), and maximum (*TMAX*) daily temperatures. Figure 4  
 236 shows, in white and gray box-plots, the  $RMSE_{val}$  and  $RMSE_{tst}$  SVR evolution for the most  
 237 elite population of the best GAparsimony iteration. In this case, GAparsimony converged in  
 238 7 generations.

239 **ANN Model:** The best ANN model converged in 4 generations with 5 features: month  
 240 (*month*), if the day was a bank holiday (*Is\_holiday*), ring temperature (*TIMP*), and the ex-  
 241 ternal (*TEXT*) and averaged (*TMED*) daily temperatures. ANN errors were only slightly  
 242 superior to those of the SVG model.

243 **XGB Model:** The best XGB model was optimized after 4 generations with 4 features:  
 244 month (*month*), day of week (*day\_of\_week*), and the external (*TEXT*) and averaged tempera-  
 245 tures (*TMED*) of the day.

246 **Ensemble Model:** Finally, the best SVR, ANN and XGB were combined to obtain an  
 247 ensemble model with an enhanced performance. The process was conducted by weighting  
 248 the predictions of each learner as follows:

$$Ensemble\_Model = (w1 * SVR + w2 * ANN + w3 * XGB) / 3.0 \quad (3)$$

249 In order to determine the weights, an optimization of  $w1$  and  $w2$  was performed by

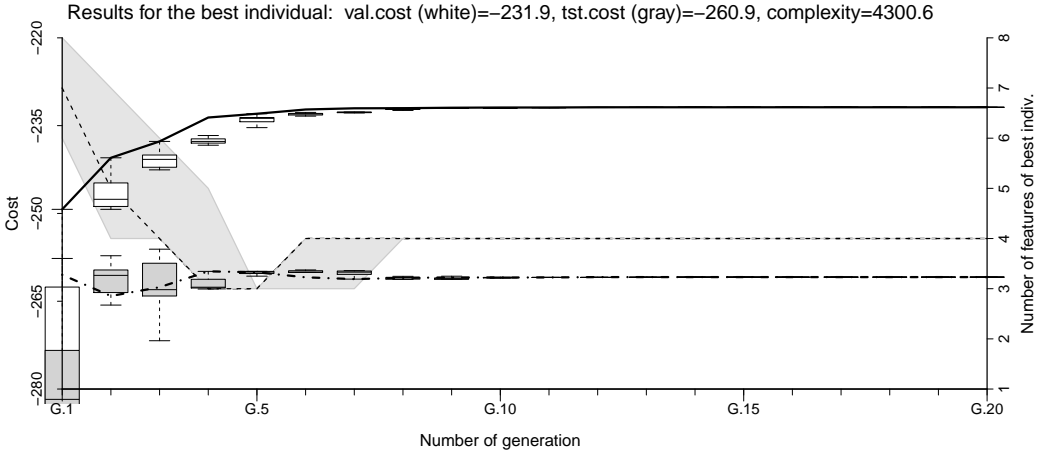


Figure 4: Evolution of the errors of the most elite solutions for SVR algorithm. White and gray box-plots represent the  $RMSE_{val}$  and  $RMSE_{tst}$  evolutions respectively and, continuous and shaded lines indicate the best individual of each population. The gray area covers the maximum and minimum number of features  $N_{FS}$  (rightaxis).

250 reducing the  $RMSE_{val}$  obtained with this equation and the previous model validation pre-  
 251 dictions. In this process,  $w_3$  was internally calculated as  $w_3 = 3 - w_1 - w_2$ .

252 The optimum model was comprised by the following weights:

$$Ensemble\_Model = (1.36 * SVR + 1.41 * ANN + 0.23 * XGB) / 3.0 \quad (4)$$

253 Table 7 shows the  $RMSE_{val}$  and  $RMSE_{tst}$  of the weighted combined model versus single  
 254 models. Error values are slightly better in the ensemble model than the best single model  
 255 (SVR Model). Complexity increases because of the number of features needed as input for  
 256 the models comprising the hybrid model; however, the variable of minimum daily temper-  
 257 ature (TMIN) was not utilized in the final model.

Table 7: Ensemble validation and test errors versus single models.

	SVR	ANN	XGB	HYBRID
$RMSE_{val}$	231.9	233.2	239.8	<b>224.82</b>
$RMSE_{tst}$	260.9	268.2	267.7	<b>257.49</b>
complexity	4	5	4	7

## 258 6. Conclusions

259 This study has demonstrated that GAparsimony is an effective and advanced method for  
 260 selecting the best parsimonious model among different forecasting methodologies, and for  
 261 adjusting internal parameters and selecting the best features as well.

262 The analysis conducted in this study took place over the course of more than three  
 263 years, and demonstrates the imperative need to optimize cooling systems before effective

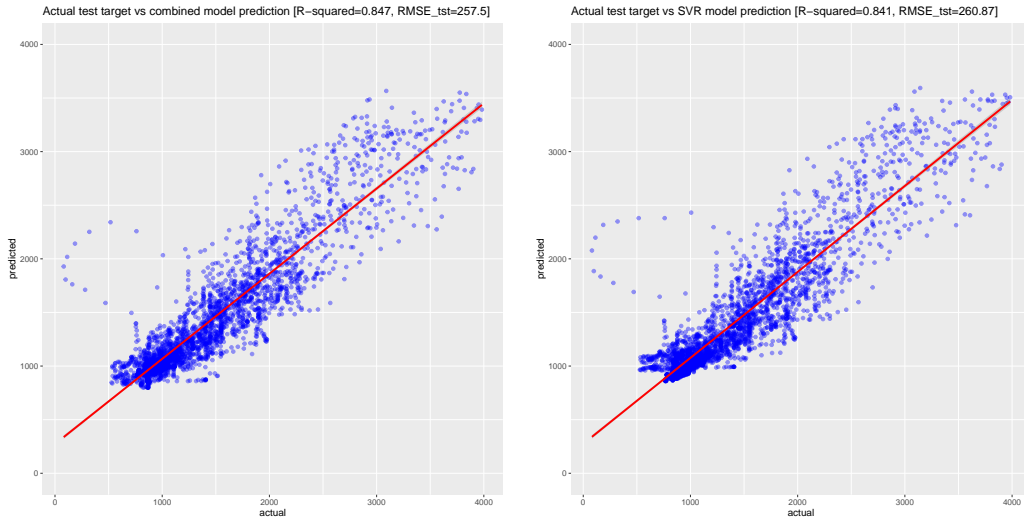


Figure 5: Ensemble and SVR combined predictions.

264 prediction models can be created, as they would then be able to learn from balanced sys-  
 265 tem data. The models obtained have similar errors and use similar features; and this fact  
 266 demonstrates that the prior optimization process was a worthwhile endeavor.

267 The final ensemble model which combines the three best parsimonious models will be  
 268 easy to maintain because information is directly available from sensors and meteorological  
 269 forecasting. The error rate has been significantly reduced compared to the initial models.  
 270 And, although it is not an insignificant error, it does facilitate forecasting that will allow  
 271 control engineers to program the chillers to supply the maximum demand for the coming  
 272 hours. In addition, with the improvements made in modulating the cooling system, the  
 273 system will be able to buffer variations not programmed into the day-to-day activity.

274 The next step in this line of research is to implement the ensemble model within the  
 275 BMS decision software, and then test and track the real response in order to validate and  
 276 measure the results.

## 277 Acknowledgements

278 We are greatly indebted to *Banco Santander* for the APPI17/04, and REGI2018/43 fellow-  
 279 ships. This study used the Beronia cluster (Universidad de La Rioja), which is supported  
 280 by FEDER-MINECO grant number UNLR-094E-2C-225.

## 281 References

## 282 References

- 283 1. Yoon, S.H., Kim, S.Y., Park, G.H., Kim, Y.K., Cho, C.H., Park, B.H.. Mul-  
 284 tiple power-based building energy management system for efficient management  
 285 of building energy. *Sustainable Cities and Society* 2018;42:462 – 470. URL: [http:](http://)

- 286 [//www.sciencedirect.com/science/article/pii/S2210670718308990](http://www.sciencedirect.com/science/article/pii/S2210670718308990). doi:<https://doi.org/10.1016/j.scs.2018.08.008>.
- 287
- 288 2. Missaoui, R., Joumaa, H., Ploix, S., Bacha, S.. Managing energy smart  
289 homes according to energy prices: Analysis of a building energy management sys-  
290 tem. *Energy and Buildings* 2014;71:155 – 167. URL: <http://www.sciencedirect.com/science/article/pii/S0378778813008335>. doi:<https://doi.org/10.1016/j.enbuild.2013.12.018>.
- 291
- 292
- 293 3. IDAE, , Fenercom, . Guía de ahorro y eficiencia energética en hospitales. *Fener-*  
294 *com* 2010;:329URL: <https://www.fenercom.com/wp-content/uploads/2010/11/Guia-de-Ahorro-y-Eficiencia-Energetica-en-Hospitales-fenercom-2010.pdf>.  
295 doi:-.
- 296
- 297 4. Shen, C., Zhao, K., Ge, J., Zhou, Q.. Analysis of building energy consumption in a  
298 hospital in the hot summer and cold winter area. *Energy Procedia* 2019;158:3735 – 3740.  
299 URL: <http://www.sciencedirect.com/science/article/pii/S1876610219309270>.  
300 doi:<https://doi.org/10.1016/j.egypro.2019.01.883>; innovative Solutions for En-  
301 ergy Transitions.
- 302 5. Saeedi, M., Moradi, M., Hosseini, M., Emamifar, A., Ghadimi, N.. Robust  
303 optimization based optimal chiller loading under cooling demand uncertainty. *Ap-*  
304 *plied Thermal Engineering* 2019;148:1081 – 1091. URL: <http://www.sciencedirect.com/science/article/pii/S1359431118353547>. doi:<https://doi.org/10.1016/j.applthermaleng.2018.11.122>.
- 305
- 306
- 307 6. Wang, L., Lee, E.W., Yuen, R.K.. Novel dynamic forecasting model for build-  
308 ing cooling loads combining an artificial neural network and an ensemble ap-  
309 proach. *Applied Energy* 2018;228:1740 – 1753. URL: <http://www.sciencedirect.com/science/article/pii/S0306261918311103>. doi:<https://doi.org/10.1016/j.apenergy.2018.07.085>.
- 310
- 311
- 312 7. Abdel-Aal, R.. Modeling and forecasting electric daily peak loads using abductive  
313 networks. *International Journal of Electrical Power & Energy Systems* 2006;28(2):133 – 141.  
314 URL: <http://www.sciencedirect.com/science/article/pii/S0142061505001390>.  
315 doi:<https://doi.org/10.1016/j.ijepes.2005.11.006>.
- 316 8. Chitsaz, H., Shaker, H., Zareipour, H., Wood, D., Amjady, N.. Short-term electric-  
317 ity load forecasting of buildings in microgrids. *Energy and Buildings* 2015;99:50 – 60.  
318 URL: <http://www.sciencedirect.com/science/article/pii/S0378778815003102>.  
319 doi:<https://doi.org/10.1016/j.enbuild.2015.04.011>.
- 320 9. Shepero, M., van der Meer, D., Munkhammar, J., Widén, J.. Residential prob-  
321 abilistic load forecasting: A method using gaussian process designed for electric  
322 load data. *Applied Energy* 2018;218:159 – 172. URL: <http://www.sciencedirect.com/science/article/pii/S030626191830299X>. doi:<https://doi.org/10.1016/j.apenergy.2018.02.165>.
- 323
- 324
- 325 10. Li, Y., Che, J., Yang, Y.. Subsampled support vector regression ensemble for  
326 short term electric load forecasting. *Energy* 2018;164:160 – 170. URL: <http://www.sciencedirect.com/science/article/pii/S0360544218317055>. doi:<https://doi.org/10.1016/j.energy.2018.08.169>.
- 327
- 328

- 329 11. Yang, Y., Che, J., Deng, C., Li, L.. Sequential grid approach based support vector  
330 regression for short-term electric load forecasting. *Applied Energy* 2019;238:1010 – 1021.  
331 URL: <http://www.sciencedirect.com/science/article/pii/S0306261919301503>.  
332 doi:<https://doi.org/10.1016/j.apenergy.2019.01.127>.
- 333 12. Jetcheva, J.G., Majidpour, M., Chen, W.P.. Neural network model ensembles  
334 for building-level electricity load forecasts. *Energy and Buildings* 2014;84:214 – 223.  
335 URL: <http://www.sciencedirect.com/science/article/pii/S0378778814006458>.  
336 doi:<https://doi.org/10.1016/j.enbuild.2014.08.004>.
- 337 13. Hsu, Y.Y., Tung, T.T., Yeh, H.C., Lu, C.N.. Two-stage artificial neural network  
338 model for short-term load forecasting. *IFAC-PapersOnLine* 2018;51(28):678 – 683.  
339 URL: <http://www.sciencedirect.com/science/article/pii/S2405896318335043>.  
340 doi:<https://doi.org/10.1016/j.ifacol.2018.11.783>; 10th IFAC Symposium on  
341 Control of Power and Energy Systems CPES 2018.
- 342 14. Bagnasco, A., Fresi, F., Saviozzi, M., Silvestro, F., Vinci, A.. Electrical con-  
343 sumption forecasting in hospital facilities: An application case. *Energy & Buildings*  
344 2015;103(Complete):261–270. doi:[10.1016/j.enbuild.2015.05.056](https://doi.org/10.1016/j.enbuild.2015.05.056).
- 345 15. Ahmad, M.W., Mourshed, M., Rezgui, Y.. Trees vs neurons: Comparison be-  
346 tween random forest and ann for high-resolution prediction of building energy con-  
347 sumption. *Energy and Buildings* 2017;147:77 – 89. URL: <http://www.sciencedirect.com/science/article/pii/S0378778816313937>. doi:<https://doi.org/10.1016/j.enbuild.2017.04.038>.
- 350 16. Singh, P., Dwivedi, P., Kant, V.. A hybrid method based on neural network  
351 and improved environmental adaptation method using controlled gaussian muta-  
352 tion with real parameter for short-term load forecasting. *Energy* 2019;174:460 – 477.  
353 URL: <http://www.sciencedirect.com/science/article/pii/S03060544219303408>.  
354 doi:<https://doi.org/10.1016/j.energy.2019.02.141>.
- 355 17. Avalos, M., Grandvalet, Y., Ambroise, C.. Parsimonious additive models. *Com-  
356 putational Statistics & Data Analysis* 2007;51(6):2851 – 2870. doi:[https://doi.org/10.  
357 1016/j.csda.2006.10.007](https://doi.org/10.1016/j.csda.2006.10.007).
- 358 18. Li, H., Shu, D., Zhang, Y., Yi, G.Y.. Simultaneous variable selection and estimation for  
359 multivariate multilevel longitudinal data with both continuous and binary responses.  
360 *Computational Statistics & Data Analysis* 2018;118:126 – 137. doi:[https://doi.org/10.  
361 1016/j.csda.2017.09.004](https://doi.org/10.1016/j.csda.2017.09.004).
- 362 19. Husain, H., Handel, N.. Automated machine learning. a paradigm shift  
363 that accelerates data scientist productivity. 2017. URL: [https://medium.com/  
364 airbnb-engineering/](https://medium.com/airbnb-engineering/).
- 365 20. Feurer, M., Klein, A., Eggenberger, K., Springenberg, J., Blum, M., Hutter, F.  
366 Efficient and robust automated machine learning. In: Cortes, C., Lawrence, N.D.,  
367 Lee, D.D., Sugiyama, M., Garnett, R., eds. *Advances in Neural Information Processing  
368 Systems* 28. Curran Associates, Inc.; 2015:2962–2970. URL: [http://papers.nips.cc/  
369 paper/5872-efficient-and-robust-automated-machine-learning.pdf](http://papers.nips.cc/paper/5872-efficient-and-robust-automated-machine-learning.pdf).

- 370 21. Sanz-Garcia, A., Fernandez-Ceniceros, J., Antonanzas-Torres, F., Pernia-Espinoza,  
371 A., Martinez-de Pison, F.J.. GA-PARSIMONY: A GA-SVR approach with feature  
372 selection and parameter optimization to obtain parsimonious solutions for predict-  
373 ing temperature settings in a continuous annealing furnace. *Applied Soft Computing*  
374 2015;35:13–28.
- 375 22. Urraca, R., Sodupe-Ortega, E., Antonanzas, J., Antonanzas-Torres, F., de Pison,  
376 F.M.. Evaluation of a novel GA-based methodology for model structure selection: The  
377 GA-PARSIMONY. *Neurocomputing* 2018;271(Supplement C):9 – 17.
- 378 23. Martinez-de Pison, F.J., Fraile-Garcia, E., Ferreiro-Cabello, J., Gonzalez, R., Pernia,  
379 A.. Searching Parsimonious Solutions with GA-PARSIMONY and XGBoost in High-  
380 Dimensional Databases. Cham: Springer International Publishing. ISBN 978-3-319-  
381 47364-2; 2017:201–210. doi:[10.1007/978-3-319-47364-2\\_20](https://doi.org/10.1007/978-3-319-47364-2_20).
- 382 24. Sanz-García, A., Fernández-Ceniceros, J., Antoñanzas-Torres, F., Martínez-de Pisón,  
383 F.J.. Parsimonious support vector machines modelling for set points in industrial  
384 processes based on genetic algorithm optimization. In: *International Joint Conference*  
385 *SOCO13-CISIS13-ICEUTE13*; vol. 239 of *Advances in Intelligent Systems and Computing*.  
386 Springer International Publishing; 2014:1–10.
- 387 25. Urraca-Valle, R., Sanz-García, A., Fernández-Ceniceros, J., Sodupe-Ortega, E.,  
388 de Pisón Ascacibar, F.J.M.. Improving hotel room demand forecasting with a hybrid  
389 GA-SVR methodology based on skewed data transformation, feature selection and  
390 parsimony tuning. In: Onieva, E., Santos, I., Osaba, E., Quintián, H., Corchado, E.,  
391 eds. *Hybrid Artificial Intelligent Systems - 10th International Conference, HAIS 2015, Bil-*  
392 *bao, Spain, June 22-24, 2015, Proceedings*; vol. 9121 of *Lecture Notes in Computer Science*.  
393 Springer. ISBN 978-3-319-19643-5; 2015:632–643. doi:[10.1007/978-3-319-19644-2\\_](https://doi.org/10.1007/978-3-319-19644-2_52)  
394 [52](https://doi.org/10.1007/978-3-319-19644-2_52).
- 395 26. Fernandez-Ceniceros, J., Sanz-Garcia, A., Antonanzas-Torres, F., de Pison, F.M.. A  
396 numerical-informational approach for characterising the ductile behaviour of the T-  
397 stub component. Part 2: Parsimonious soft-computing-based metamodel. *Engineering*  
398 *Structures* 2015;82:249 – 260. doi:[http://dx.doi.org/10.1016/j.engstruct.2014.](http://dx.doi.org/10.1016/j.engstruct.2014.06.047)  
399 [06.047](http://dx.doi.org/10.1016/j.engstruct.2014.06.047).
- 400 27. Antonanzas-Torres, F., Urraca, R., Antonanzas, J., Fernandez-Ceniceros, J., de Pison,  
401 F.M.. Generation of daily global solar irradiation with support vector machines for  
402 regression. *Energy Conversion and Management* 2015;96:277 – 286. doi:[http://dx.doi.](http://dx.doi.org/10.1016/j.enconman.2015.02.086)  
403 [org/10.1016/j.enconman.2015.02.086](http://dx.doi.org/10.1016/j.enconman.2015.02.086).
- 404 28. Sanz-Garcia, A., Fernandez-Ceniceros, J., Antonanzas-Torres, F., Pernia-Espinoza,  
405 A., Martinez-de Pison, F.. Ga-parsimony. *Appl Soft Comput* 2015;35(C):13–28.  
406 URL: <https://doi.org/10.1016/j.asoc.2015.06.012>. doi:[10.1016/j.asoc.2015.](https://doi.org/10.1016/j.asoc.2015.06.012)  
407 [06.012](https://doi.org/10.1016/j.asoc.2015.06.012).
- 408 29. Martínez-De-Pisón, F.J.. GAparsimony: GA-based optimization R package for  
409 searching accurate parsimonious models.; 2017. URL: [https://github.com/jpison/](https://github.com/jpison/GAparsimony)  
410 [GAparsimony](https://github.com/jpison/GAparsimony); R package version 0.9-1.